

Mitochondrial miRNA Determines Chemoresistance by Reprogramming Metabolism and Regulating Mitochondrial Transcription



Song Fan^{1,2,3}, Tian Tian⁴, Weixiong Chen², Xiaobin Lv^{5,6}, Xinyuan Lei², Hanqing Zhang², Sheng Sun⁷, Lei Cai³, Guokai Pan², Lile He³, Zhanpeng Ou², Xinyu Lin², Xinhui Wang³, Matthew Francis Perez³, Zhiming Tu³, Soldano Ferrone³, Bakhos A. Tannous⁸, and Jinsong Li^{1,2}

Abstract

miRNAs that translocate from the nucleus to mitochondria are referred to as mitochondrial microRNAs (mitomiR). mitomiRs have been shown to modulate the translational activity of the mitochondrial genome, yet their role in mitochondrial DNA (mtDNA) transcription remains to be determined. Here we report that the mitomiR-2392 regulates chemoresistance in tongue squamous cell carcinoma (TSCC) cells by reprogramming metabolism via downregulation of oxidative phosphorylation and upregulation of glycolysis. These effects were mediated through partial inhibition of mtDNA transcription by mitomiR-2392 rather than through translational regulation. This repression required specific miRNA-mtDNA base pairing and Argonaute 2. mitomiR-2392 recognized target sequences in the H-strand and partially inhibited polycistronic mtDNA transcription in a cell-specific manner. A retrospective

analysis of TSCC patient tumors revealed a significant association of miR-2392 and regulated mitochondrial gene expression with chemosensitivity and overall survival. The clinical relevance of targeted mitochondrial genes was consistently validated by The Cancer Genome Atlas RNA sequencing in multiple types of cancer. Our study revealed for the first time the role of mitomiR in mtDNA transcription and its contribution to the molecular basis of tumor cell metabolism and chemoresistance.

Significance: These findings uncover a novel mechanism by which mitomiRNA regulates mitochondrial transcription and provide rationale for use of mitomiRNA and mtDNA-encoded genes to predict chemosensitivity and patient clinical prognosis.

¹Department of Oral and Maxillofacial Surgery, Sun Yat-Sen Memorial Hospital of Sun Yat-Sen University, Guangzhou, China. ²Guangdong Provincial Key Laboratory of Malignant Tumor Epigenetics and Gene Regulation of Sun Yat-Sen Memorial Hospital, Guangzhou, China. ³Department of Surgery, Massachusetts General Hospital, Harvard Medical School, Boston, Massachusetts. ⁴Department of Neurobiology, Key Laboratory of Human Functional Genomics of Jiangsu, Nanjing Medical University, Nanjing, Jiangsu, China. ⁵Markey Cancer Center, The University of Kentucky, College of Medicine, Lexington, Kentucky. ⁶Nanchang Key Laboratory of Cancer Pathogenesis and Translational Research, Center Laboratory, the Third Affiliated Hospital, Nanchang University, Nanchang, China. ⁷Massachusetts General Hospital Cancer Center, Harvard Medical School, Boston, Massachusetts. ⁸Experimental Therapeutics and Molecular Imaging Lab, Department of Neurology, Massachusetts General Hospital and Harvard Medical School, Boston, Massachusetts.

Note: Supplementary data for this article are available at Cancer Research Online (<http://cancerres.aacrjournals.org/>).

S. Fan, T. Tian, W. Chen, and X. Lv contributed equally to this work.

Corresponding Authors: Soldano Ferrone, Massachusetts General Hospital, Harvard Medical School, 55 Fruit Street, Boston, MA 02114. Phone: 617-726-6087; Fax: 617-726-8623; E-mail: sferrone@mgh.harvard.edu; and Jin-song Li, Guangdong Provincial Key Laboratory of Malignant Tumor Epigenetics and Gene Regulation of Sun Yat-Sen Memorial Hospital, Guangzhou 510120, China. Phone: 86-020-81332099; E-mail: lijinsong1967@163.com

doi: 10.1158/0008-5472.CAN-18-2505

©2019 American Association for Cancer Research.

Introduction

The "Warburg effect" was discovered in the 1920s and consists of an increase in glycolysis that is maintained under high oxygen tension conditions ("aerobic glycolysis") and gives rise to enhanced lactate production (1). The enhanced glucose uptake for glycolytic adenosine triphosphate (ATP) generation and anabolic reactions that convey an advantage to cancer cells have been well studied. First, cancer cells can live under fluctuating oxygen tension conditions under the condition of aerobic glycolysis. Second, cancer cells generate bicarbonic and lactic acids through aerobic glycolysis. Third, tumors can generate NADPH to defend against a hostile microenvironment and chemotherapeutic agents (2). Fourth, cancer cells use intermediates of the glycolytic pathway for anabolic reactions (2). Metabolic alterations in cancer cells are intricately linked to the principal hallmarks of cancer. Warburg originally hypothesized that cancer cells develop a defect in their mitochondria that leads to impaired aerobic respiration and a subsequent reliance on glycolytic metabolism. However, numerous studies have shown that mitochondrial function is not impaired in most cancer cells, and the presence of a dynamic equilibrium between glycolytic and oxidative phosphorylation (OXPHOS) has been found in different types of cancer cells (3, 4). Therefore, aerobic glycolysis and mitochondria function together during cancer progression, and this metabolic flexibility allows a given cell to alternate

between aerobic glycolysis and OXPHOS to arrest the traits of malignant phenotypes, such as chemoresistance (5). However, the precise mechanisms of metabolic reprogramming remain elusive.

Mitochondria are dynamic double-membrane organelles that generate ATP via OXPHOS and are at the heart of other critical metabolic pathways. Mammalian mitochondrial DNA (mtDNA) is approximately 16.6 kb and encodes 13 mRNAs for key subunits of the OXPHOS pathway (6). Twelve OXPHOS mitochondrial genes are sequentially transcribed from the H-strands, and only ND6 is transcribed from the L-strand (7). Mitochondrial RNA synthesis and processing is a highly regulated, coordinated, multistep process, although it has not been fully characterized (8). mtDNA transcription is entirely dependent on three factors encoded by nuclear genes, namely, mitochondrial RNA polymerase (POLRMT), mitochondrial transcription factor B2 (TFB2M), and mitochondrial transcription factor A (TFAM; refs. 9, 10). There is an ongoing debate as to whether all three of these components are required for basal, promoter-specific transcription initiation (11, 12), and it has also been suggested that there may be differential regulation by the mitochondrial transcription factors TFAM and TFB2M (13, 14). Therefore, these data suggest the possibility that other molecules trigger mitochondrial transcription, but this hypothesis needs to be verified.

The biological functions and mechanisms of miRNAs have been widely studied in eukaryotic cells. The primary miRNA machinery is known to act in the cytoplasm through binding to target mRNAs via partial base-pairing within RNA-induced silencing complexes (RISC) and regulation of both mRNA stability and translation (15, 16). In addition to their primary function in translational repression, miRNAs have also been implicated in enhancing (17) or inhibiting transcription under specific cellular conditions (18–20). Furthermore, miRNAs have also been detected in membrane-bound compartments, such as secreted vesicles and mitochondria (21–26), and mitochondrial miRNAs have been termed mitochondrial microRNAs (mitomiR). Both mitomiRs and the slicing-competent Argonaute 2 (AGO2) protein have been investigated for their important roles in translation of mitochondrial transcripts (25, 26). However, the transcriptional regulation effects of mitomiRs on the mitochondrial genome remain unknown.

Here, we investigated the function of mitomiRs in chemoresistance and metabolic balance in tongue squamous cell carcinoma (TSCC). Notably, we found that one of the mitomiRs, miR-2392, could reverse chemoresistance and reprogram metabolism by partially regulating mitochondrial gene transcription.

Materials and Methods

Cell culture

The human TSCC cell lines CAL-27 and SCC-9 were purchased from the ATCC. The stable cisplatin-resistant lines CAL-27-res and SCC-9-re were established by exposing CAL-27 or SCC-9 cells to cisplatin (Sigma), ranging from 10^{-7} M to 10^{-5} M (27). All cell lines were routinely tested for *Mycoplasma*, and the genetic identity of the cell lines was confirmed by short tandem repeat (STR) profiling (ATCC). The cell lines were used for experiments within 10 passages after thawing. The establishment of primary cell cultures from surgical specimens was performed as previously described (28). The primary cultured cells were used for isolation of mitochondria within five passages.

Isolation of mitochondrial, cytoplasmic, and nuclear fractions

Subcellular fractions were prepared as described previously (29, 30). Briefly, the cells were washed twice with cold PBS, and the pellet was suspended in 0.2 mL of lysis buffer containing a protease inhibitor cocktail. Then, the cells were homogenized, followed by centrifugation twice at 750 g for 5 minutes at 4°C to collect the nuclei and debris. The mitochondria-enriched heavy membrane pellet was collected with further centrifugation at $10,000 \times g$ for 15 minutes at 4°C whereas the supernatants were collected as the cytosolic fractions.

Quantification of mtDNA and miR-2392

For quantification of mtDNA, we used a pair of primers that target the ND5 gene for qPCR analysis. To quantify nDNA, we used a pair of primers that target the nuclear PECAM1 gene for qPCR analysis. According to The Cancer Genome Atlas (TCGA) database, ND5 and PECAM1 do not have any genetic alteration in head and neck cancer.

To quantify the copy number of miR-2392 per nucleus or per mitochondrial genome, we generated a standard curve by RT-qPCR using a series dilution of synthetic miR-2392 from Ribobio and then performed quantitative analysis of miR-2392 in whole-cell lysate or purified mitochondria.

miRNA profiles

The miRNA microarrays were performed by Shanghai Biotechnology with Agilent human miRNA (8*60K) V19.0 microarrays. The detected RNA included cytosolic RNA, mitochondrial RNA, and total RNA.

Evaluation of mtDNA transcripts stability

The effect of miR-2392 on the stability of mtDNA-encoded transcripts was determined by adding the transcriptional inhibitor actinomycin D to the cultures at a final concentration of 5 µg/mL. After 24 hours, either control or miR-2392 mimics transfection, the total RNA and mitochondrial RNA was isolated at indicated times under actinomycin D treatment and processed for qRT-PCR.

RNA immunoprecipitation

RNA immunoprecipitation was performed using a Magna RIP RNA-Binding Protein Immunoprecipitation Kit (17-700; Millipore) according to the manufacturer's instructions. Briefly, mitochondria were washed twice with PBS at room temperature followed by IP lysis buffer for 20 minutes at 4°C. When the complex was removed from the dish, it was centrifuged for 15 minutes at $12,000 \times g$ and 4°C. The supernatant was divided into two parts, and then, anti-AGO2 antibody (Abcam, ab57113) and IgG were added, followed by rotation at 20 rpm for 1 hour. Protein beads were added to each tube followed by rotation at 20 rpm for 0.5 hour. A magnetic frame was applied to remove the supernatant, followed by three washes with a lysis buffer. Protease K and RNase inhibitor were added to the lysis buffer, followed by rotation for 30 minutes at 55°C to remove the protein. TRIzol LS was added to the remaining solution, and RNA was then extracted from it. qRT-PCR was applied to assess miR-2392 and miR-135b-5p expression in the immunocomplex.

Biotinylated pull-downs assay

Pull-downs of miR-2392 targets were carried out as previously described, with slight modifications. Briefly, 80 nmol of biotin-labeled oligos were used to transiently transfect CAL-27 cells and

the mitochondria were isolated and fixed in 1% formaldehyde at 37 °C for 10 minutes, followed by crosslinking reaction and sonication to shear the DNA. Then, the lysate was centrifuged, followed by binding with M-280 Streptavidin Dynabeads. The binding of DNA fragments to miRNAs was analyzed with qPCR.

Luciferase assay

Dual luciferase assays were performed at 48 hours after plasmid transfection using the Luciferase Assay Kit from Promega. SD was based on triplicated experiments. The miR-2393 targeting sequence was synthesized and cloned into *Hind*III restrict endonuclease of the pGL3-Control plasmid.

Tumor xenografts

A TSCC xenograft mouse model was used to evaluate *in vivo* cisplatin sensitivity. When BALB/c-nu mice were 4 to 6 weeks old, a 5×10^6 cells resuspension in 150 μ L of PBS was injected subcutaneously into the flanks of the nude mice ($n = 6$ for each group). One week after implantation, when the tumor became palpable at a size of approximately 2 mm in diameter, cisplatin (5 mg/kg) or equivolume saline was administered via intraperitoneal injection every 3 days from days 8 to 32.

Patients and samples

Specimens of locally advanced TSCCs ($n = 115$) were obtained before neoadjuvant chemosensitivity between January 1, 2004, and December 31, 2010. The patients with locally advanced resectable TSCC (stage III or IVA) underwent one or two cycles of neoadjuvant chemotherapy (TPF induction chemotherapy; ref. 31), and the tumor response to neoadjuvant chemotherapy was assessed by CT/MRI imaging studies prior to radical resection.

Study approval

Patient study was conducted in accordance with the principles of the Declaration of Helsinki. Ethics approval was provided by the Sun Yat-sen University Committee for Ethical Review of Research Involving Human Subjects. Patients with TSCC were identified and provided written informed consent under 20141114 from Sun Yat-sen Memorial Hospital. The animal experiments were performed in accordance with the Institutional Authorities' guidelines and formally approved by the Animal Ethics Committee of Sun Yat-sen University.

Statistical analysis

Experiments were carried out with three or more replicates. Statistical analyses were performed using Student *t* test unless otherwise stated. Values with $P < 0.05$ are considered statistically significant.

Additional methods

Addition methods are provided in the Supplementary Information.

Results

mitomiRs expression in TSCC cisplatin-resistant cells and their parental cell line

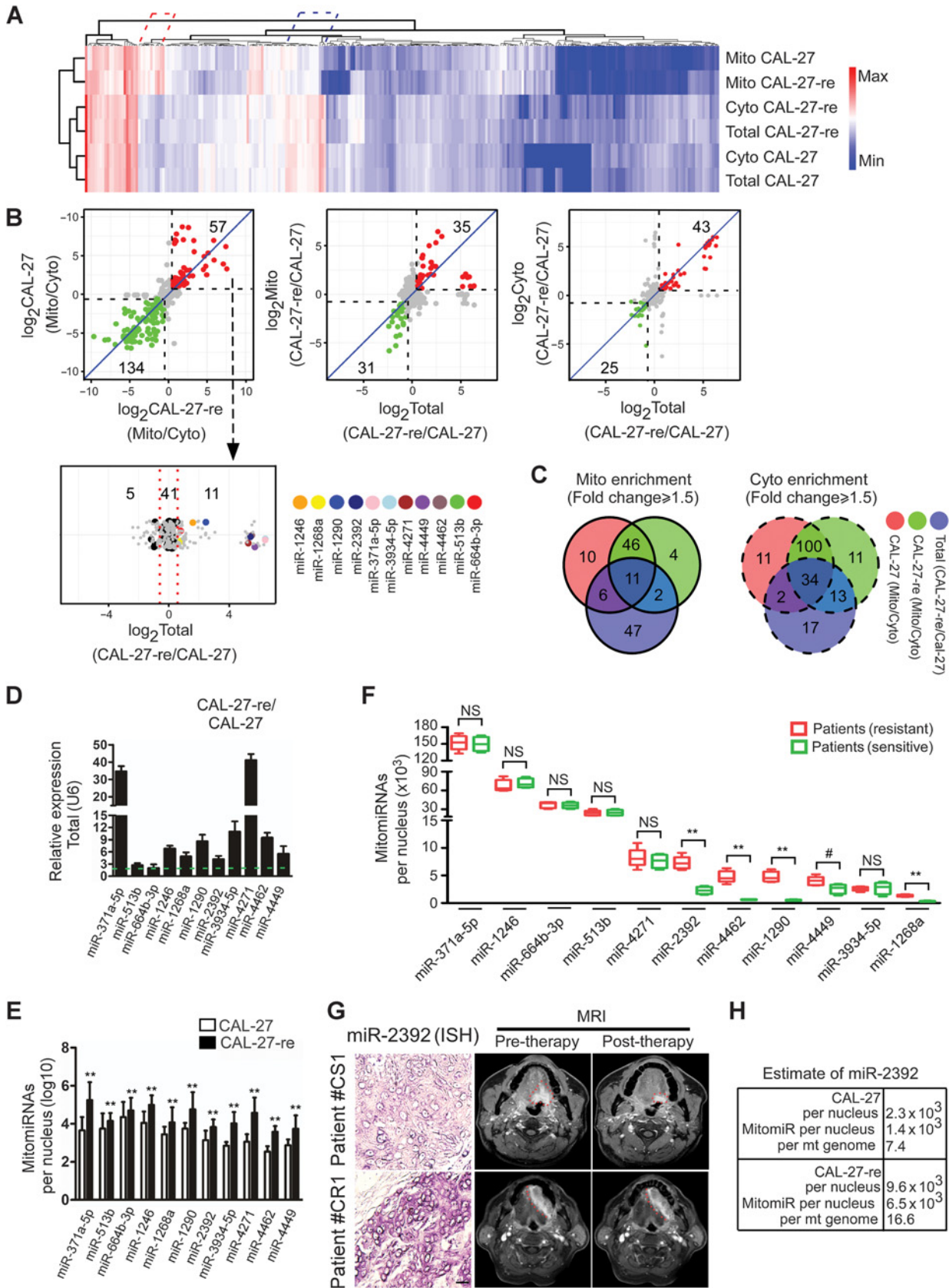
To investigate mitomiR regulation of mitochondrial OXPHOS and chemoresistance, we analyzed the differential expression of mitomiRs in TSCC cisplatin-resistant cells and their parental cells. We extracted RNAs from the mitochondria,

cytoplasm, and total cells of the cisplatin-resistant CAL-27 cells (CAL-27-re; ref. 27) and parent cell lines. We first confirmed the purity of the mitochondria at the protein, mRNA, and DNA levels (Supplementary Fig. S1A–S1C). Then, microarray approach was performed and 263 miRNAs were detected in all six components with significantly upregulated or downregulated clusters (Fig. 1A). We identified 57 mitochondria-enriched miRNAs and 134 cytoplasm-enriched miRNAs in both cell lines when comparing miRNAs in the mitochondria and cytosolic fractions (≥ 1.5 -fold; Fig. 1B). Compared with the total miRNA, 35 mitomiRs and 43 cytoplasmic miRNAs were upregulated in CAL-27-re cells, whereas 31 mitomiRs and 25 cytoplasmic miRNAs were upregulated in CAL-27 cells (≥ 1.5 fold; Fig. 1B). Moreover, 11 mitomiRs and 34 cytoplasmic miRNAs were found upregulated in the resistant cells (≥ 1.5 fold; Fig. 1B and C; Supplementary Fig. S1D and S1E).

Quantification of mitomiRs expression in the mitochondria of TSCC cells

Because isolated mitochondria are often contaminated with cytoplasmic RNA (25), we applied RNase T1 (RN T1) and micrococcal nuclease (MNase) to treat the mitochondria before RNA extraction. We found that both nuclear U6 and cytoplasmic GAPDH mRNA were largely removed from purified mitochondria, and any residual amounts could be fully degraded by a combination of RN T1 and MNase whereas mitochondrial 16S rRNA and 12S rRNA present a similar nuclease sensitivity (Supplementary Fig. S2A).

Next, we validated our microarray data in our purified mitochondria using quantitative real-time PCR (qRT-PCR). We confirmed that 11 mitomiRs were mainly localized in the mitochondria of both cells (Supplementary Fig. S2B) and were upregulated in CAL-27-re cells compared with CAL-27 cells (Fig. 1D). The other 34 cytoplasmic miRNAs were predominantly localized to cytoplasm (Supplementary Fig. S2C). Then, we wanted to quantitatively determine the levels of 11 mitomiRs in the mitochondria by using the standard curve (Supplementary Fig. S2D). As a cancer cell may contain more than one nucleus, we determined the copy number of nuclear DNA (nDNA) by qPCR to calculate the number of mitomiRs molecules per nuclear genome (Fig. 1E). However, the expression profiles of these 11 mitomiRs were different in the other paired cells; three mitomiRs showed no significant difference in SCC-9 and SCC-9-re cells (Supplementary Fig. S2E and S2F). In an attempt to identify these mitomiRs required for cisplatin resistance, we tested primary cultured cells from chemosensitive and chemoresistant patients (Supplementary Table S1) for further screening. From the 11 significant expressions of mitomiRs validated in TSCC cells, five mitomiRs were significantly upregulated in the chemoresistant patients whereas miR-2392 presented the highest copy number (Fig. 1F). Importantly, the expression of miR-2392 determined by locked nucleic acid (LNA)-based ISH was markedly increased in chemoresistant patient tumors (Fig. 1G; Supplementary Fig. S2G). Interestingly, analyses of GEO databases showed that miR-2392 expression was also significantly upregulated in cisplatin-resistant pancreatic ductal adenocarcinoma cells (Supplementary Fig. S2H). Then, we focused on mitomiR-2392 in the cellular system. We also determined the ratio of mitochondrial and nuclear DNA in our cell models, revealing a ratio of 189 in CAL-27 cells and 391 in CAL-27-re cells (Supplementary Fig. S2I), which is similar to the previous studies that cisplatin-



resistant cells had a greater number of mitochondria than parental cells (32, 33). Finally, we determined the amount of miR-2392 in the mitochondria, revealing 1.4×10^3 and 6.5×10^3 mitomiR-2392 per nDNA in CAL-27 and CAL-27-re cells, respectively; and $1.4 \times 10^3/189 = 7.4$ per mtDNA in CAL-27 and $6.5 \times 10^3/391 = 16.6$ per mtDNA in CAL-27-re; and a total amount of $1.4 \times 10^3/2.3 \times 10^3 = 60.9\%$ in CAL-27 mitochondria whereas $6.5 \times 10^3/9.6 \times 10^3 = 67.7\%$ in CAL-27-re mitochondria (Fig. 1H). Therefore, we concluded that miR-2392 is a mitomiR and increased in cisplatin-resistant TSCC cells and tumors.

mitomiR-2392 regulate cisplatin resistance by reprogramming metabolism

Studies have shown a shift from mitochondrial respiration to glycolysis in chemoresistant cells (5, 34). We first found reduced activity of mitochondrial complexes and ATP level along with elevated mitochondrial superoxide (MitoSOX) and lactate production in TSCC-resistant cells (Supplementary Fig. S3A–S3E). Next, we wondered whether mitomiRs could regulate cisplatin resistance by rebuilding metabolic balance. Among the 11 identified mitomiRs, we focused on miR-2392 as it had the highest and most significant expression in the tumor screening and has been implicated in the prediction or modulation of tumor behavior (35, 36). We also found that miR-2392 predominantly localized in the mitochondria and was upregulated in SCC-9-re cells compared with parental cells (Supplementary Fig. S2E and S2F; Supplementary Fig. S4A). miRNA mimics are artificial double-stranded miRNA-like RNA fragments designed for gene-silencing approaches, whereas miRNA sponges are RNA transcripts containing multiple high-affinity binding sites that associate with and sequester-specific miRNAs to reduce their expression and prevent them from interacting with their target mRNAs (16, 25, 27). First, we found that 80 nmol miR-2392 mimic significantly increased miR-2392 expression in CAL-27 and SCC-9 cells, whereas stable expression of a miR-2392 sponge dramatically reduced miR-2392 in CAL-27-re and SCC-9-re cells (Supplementary Fig. S4B). Furthermore, we found that miR-2392 mimic reduced apoptosis under cisplatin treatment in CAL-27 and SCC-9 cells, whereas downregulation of miR-2392 increased apoptosis in CAL27-re and SCC9-re cells (Fig. 2A). Meanwhile, some other mitomiRs, including miR-371a-5p, miR-4271, miR-4462, miR-1290, and miR-4449, had no effect on apoptosis in both TSCC cell lines (Supplementary Fig. S4C). In validating whether miR-2392 had an effect on metabolic balance, we

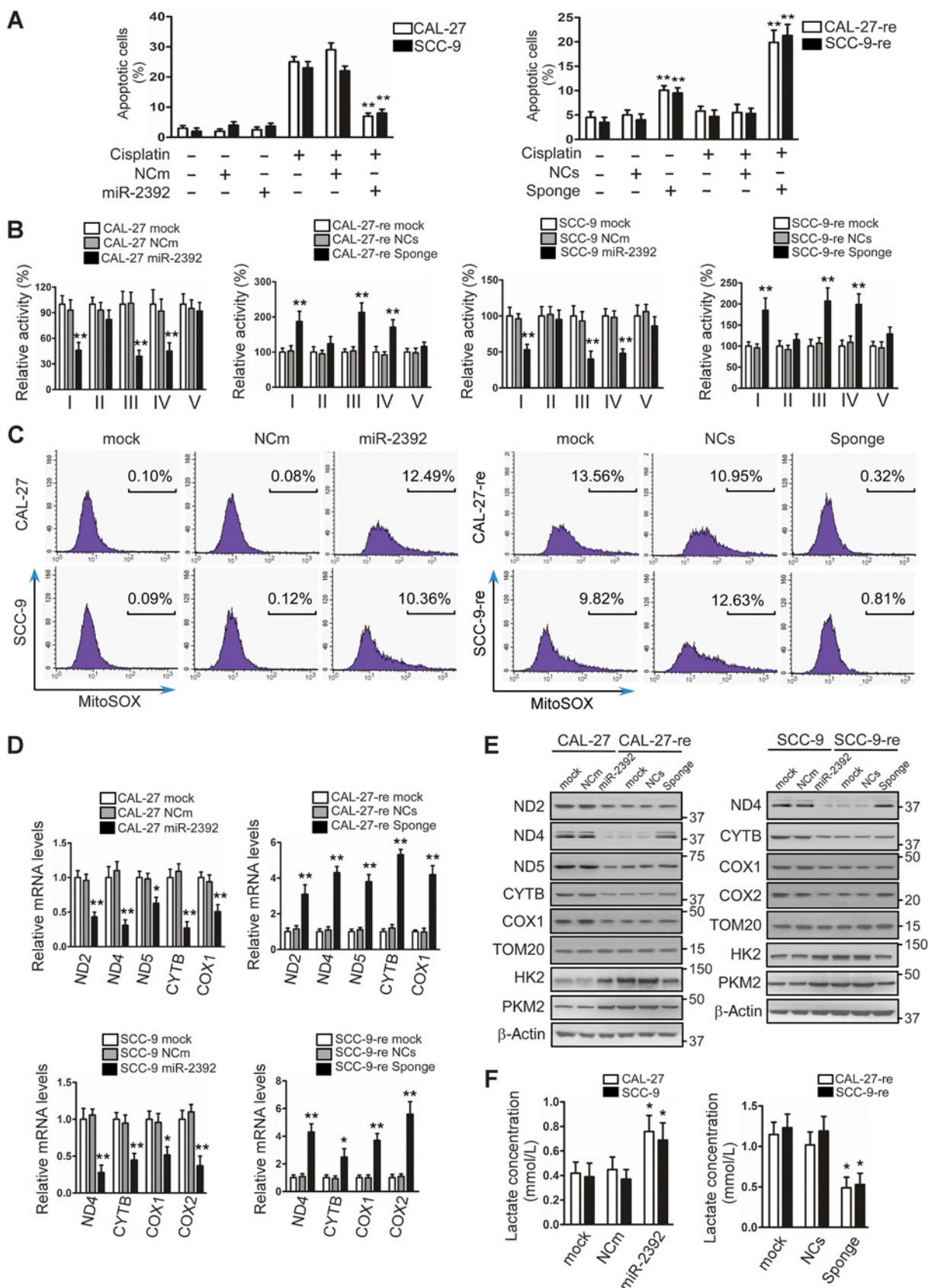
found that overexpression of miR-2392 downregulated the activity of mitochondrial complexes I, III, and IV in both CAL-27 and SCC-9 cells (Fig. 2B), whereas mitochondrial ROS (Fig. 2C; Supplementary Fig. S4D) were significantly increased, and ATP production was reduced (Supplementary Fig. S4E). However, miR-2392 downregulation restored the activities of mitochondrial complexes and ATP level (Fig. 2B; Supplementary Fig. S4E), and decreased mitochondrial ROS levels (Fig. 2C; Supplementary Fig. S4D) in both resistant cells lines. To further evaluate whether mitomiRs and miR-2392 could regulate mitochondrial gene expression, we focused on 13 polypeptides encoded by mtDNA, all of which are core components of the mitochondrial respiration-OXPHOS system. Surprisingly, we found that miR-2392 mimic significantly reduced ND2, ND4, ND5, CYTB, and COX1 mRNA and protein expression in CAL-27 cells and ND4, CYTB, COX1, and COX2 mRNA and protein expression in SCC-9 cells (Fig. 2D and E). By contrast, silencing miR-2392 led to a reverse effect on resistant cells (Fig. 2D and E). The other genes of the 13 polypeptides were not significantly changed by modulation of miR-2392 expression (Supplementary Fig. S4F). The differential expression of 13 polycistronic transcripts encoded by mtDNA were also found by RNA-sequencing data of TCGA tumors (37). In addition, lactate production (Fig. 2F) and the specific glycolytic enzymes HK2 and PKM2 (38) were also upregulated by overexpression miR-2392 in CAL-27 and SCC-9 cells, and reduced by silencing miR-2392 expression in resistant cells (Fig. 2E). Moreover, we explored the use of a heterogeneous mixture of siRNAs against mtDNA-encoded CYTB or COX1 to determine their contributions to mitochondrial function and cell apoptosis. We found that siRNA treatment led to the specific downregulation of mitochondrial targets at both the mRNA (Supplementary Fig. S4G) and protein (Supplementary Fig. S4H) levels. As expected, ROS levels were significantly increased in siRNA-treated CAL-27 and SCC-9 cells, whereas apoptosis was attenuated by siRNAs in cisplatin-treated cells (Supplementary Fig. S4I and S4J). Overall, our data suggest that the mitomiR-2392 regulates chemoresistance by rebuilding the balance between mitochondrial respiration-OXPHOS and glycolysis, and that potential mechanism contributes to transcriptional regulation rather than translation (25, 26).

mitomiR-2392 partially regulates mitochondrial gene transcription

To begin exploring these possibilities, we first investigated whether miR-2392 could regulate mitochondrial replication

Figure 1.

mitomiR expression in TSCC cisplatin-resistant cells and their parental lines. **A**, Hierarchical clustering of relative miRNA expression in the mitochondrial fraction (Mito), cytoplasmic fraction (Cyto), and total cell homogenate (Total) of CAL27 and CAL-27-re cells. miRNA expression \log_2 -fold change over blue to red color gradation is based on the ranking of each condition from minimum (blue) to maximum (red). A total of 263 miRNA genes are depicted. Red cluster, significantly upregulated miRNAs in the mitochondria. Blue, significantly downregulated miRNAs in the mitochondria. **B**, \log_2 -fold relative miRNA probe distribution showing differential miRNA expression from Mito/Cyto (top left), Mito (top middle), or Cyto (top right) compared with Total miRNA in CAL-27 and CAL-27-re cells. Genes in the right upper quadrant exhibited upregulated expression and in the left lower quadrant exhibited downregulated expression. In CAL-27-re cells compared with CAL-27 cells, 11 mitomiRs were upregulated and five mitomiRs were downregulated, whereas 41 mitomiRs showed no differences (bottom; fold change ≥ 1.5). **C**, Venn diagrams depicting overlapping miRNAs that are enriched in mitochondria and upregulated in CAL-27-re cells (left) and cytoplasmic-enriched miRNAs upregulated in CAL-27-re cells (right; fold change ≥ 1.5). **D**, qRT-PCR results showing that 11 mitomiRs were upregulated in CAL-27-re cells compared with their levels in CAL-27 cells. U6 served as the internal control for the total RNA analysis. **E**, Quantification of 11 mitomiRs per CAL-27 and CAL27-re nucleus. **F**, Quantification of 11 mitomiRs per nucleus of primary cultured cells from chemosensitive and chemoresistant patients. **G**, Representative images of miR-2392 expression of tissue specimens (left) and tumor response (right) in patients with chemosensitive (CS) and chemoresistant (CR) tumors. Bar, 20 μm . **H**, Quantification of miR-2392 per CAL-27 and CAL-27-re nucleus or per mitochondrial genome. NS, no significance; #, $P < 0.05$; **, $P < 0.001$, two-tailed Student *t* tests.



and the expression of the mitochondrial transcription factors POLRMT, TFB2M, and TFAM. However, we found that miR-2392 had no effect on mtDNA copy number and mitochondrial transcription factor expression in CAL-27 and CAL-27-re cell lines (Supplementary Fig. S5A and S5B). We were curious as to whether miR-2392 affects mitochondrial transcript stability. However, no significant reductions in half-life were observed with mitomiR-2392-targeted mtDNA-encoded ND2, ND4, ND5, CYTB, and COX1 in CAL-27 cells or ND4, CYTB, COX1, and COX2 in SCC-9 cells, which were treated with actinomycin D along with transfection of miR-2392 mimics (Fig. 3A).

Given the previous observations that miRNAs were reported to be involved in transcriptional regulation of nuclear genes through complementary gene promoters (17–20), we reasoned that mitomiR-2392 might account for mitochondrial transcription that has yet to be demonstrated. Therefore, we analyzed human mitochondrial genome promoters and the whole gene body, including H- and L-strands, using computational target prediction (RNAhybrid), and found that there were optimal binding sites for miR-2392 from 4379 to 4401 in the H-strand (Fig. 3B and C; Supplementary Table S2). Frequent mutations have been reported in mtDNA (39), but we did not find any changed sequences in the miR-2392 target sites in CAL-27 and CAL27-re cell lines (Supplementary Table S3). A WebLogo analysis of the multiz alignment of 12 mammalian species further revealed that this region of the H strand is highly conserved in six primates, suggesting that the target sequence is of biological importance in primates (Fig. 3D).

Then, we validated the specific effects of each segment of complementarity on gene silencing, and we designed mutant miRNA mimics that contained three base changes in the 3' region of miR-2392 (3'-mut), two base changes in the middle region of complementarity (mid-mut), or seven base changes in the 5' region of complementarity (5'-mut; Fig. 3E; Supplementary Fig. S5C). Another two mitomiRNAs, mitomiR-513b and mitomiR-1290, without optimal binding sites for mtDNA were selected as the negative controls (Supplementary Table S2). We used qRT-PCR to measure the expressions of ND2, ND4, ND5, CYTB, and COX1 mRNA in CAL-27 cells following treatment with each mutant miRNA mimic. Meanwhile, ND4, CYTB, COX1, and COX2 were detected in SCC-9 cells. Mutating the seed sequence of the 3' region and the middle region did not significantly affect silencing activity, while mutating the 5' region of complementarity abolished silencing (Fig. 3F; Sup-

plementary Fig. S5D). In addition, mitomiR-513b and mitomiR-1290 had no effect on gene expression. Moreover, miR-2392 is enriched in the mitochondria but is also found in the nucleus with limited expression (Fig. 3G) in CAL-27 cells. To test whether miR-2392 has the potential to regulate nuclear gene transcription, we compared the mRNA profile of CAL-27 and CAL-27-re cells and predicted the binding sites within 1 kb upstream of the transcription start site (TSS) of the first 50 downregulated mRNAs in CAL-27-re cells (Table S2). Notably, the sequence analysis revealed that miR-2392 also had optimal binding sites at the nuclear genes RGCC and STAT1, but miR-2392 had no effect on RGCC and STAT1 expression (Supplementary Fig. S5E and S5F). These results demonstrated that mitomiR-2392 partially regulates mitochondrial transcriptional activities based on specific seed sequences, but the mechanism that determines miRNA target recognition may be different from that in nucleus.

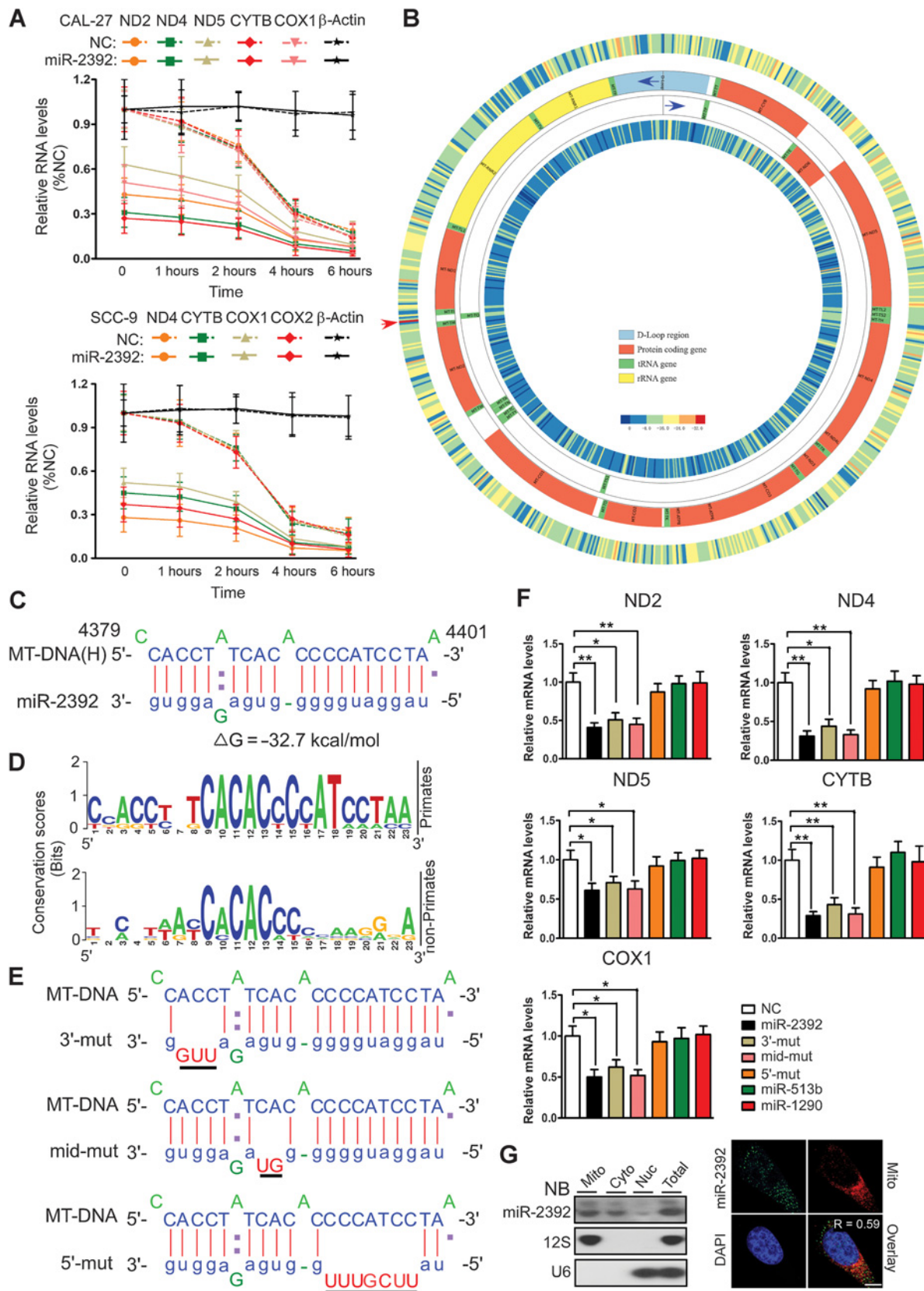
mitomiR-2392 regulates mitochondrial gene transcription through an AGO2-dependent manner

To understand how mitomiR-2392 represses mitochondrial transcription, we first asked if there is interaction of miR-2392 and AGO2 in our cellular system since Argonaute-miRNA complex has been demonstrated to modulate nuclear gene transcription (19, 20) and AGO2 has been revealed in the mitochondria and regulates mitochondrial gene expression at the translational level in association with miRNA (22, 25).

We first validated the presence of AGO2 in mitochondria in CAL-27 and CAL-27-re cells (Fig. 4A and B). We then found that miR-2392 was coimmunoprecipitated by AGO2 in mitochondrial pellet, while the occupancy of miR-2392 in CAL-27-re cells was significantly higher than in CAL-27 cells or the occupancy of cytoplasmic miR-135b-5p (Fig. 4C). Moreover, we used biotin-labeled miR-2392 and mutants to identify the association between miR-2392 and AGO2 and validate the base-pair binding between miR-2392 and specific regulatory regions of mtDNA (Supplementary Fig. S6A). We found that AGO2 coimmunoprecipitates with both miR-2392 and its negative control (Fig. 4D), whereas biotin-labeled miRNA coimmunoprecipitates with AGO2 (Supplementary Fig. S6B). Importantly, the occupancy of miR-2392 was significantly higher in the mtDNA region (4379–4401) rather than at other poorly matched binding site (10104–10126), and the mutation decreased the recruitment of miR-2392, particularly, in the 5' end mutants (Fig. 4E). Furthermore, we found that the

Figure 2.

mitomiR-2392 regulates cisplatin resistance and metabolism reprogramming. **A**, Flow cytometry analysis showing that CAL-27 or SCC-9 cells transfected with miR-2392 mimic resist cisplatin-induced apoptosis, whereas CAL-27-re or SCC-9-re cells with stable expression of a miR-2392 sponge were sensitive to cisplatin-induced apoptosis. **B**, The activity of mitochondrial respiratory chain complex I, III, and IV was significantly downregulated in CAL-27 and SCC-9 cells by transfection with miR-2392 mimic. Meanwhile, the activity of mitochondrial respiratory chain complex I, III, and IV subunits was restored in CAL-27-re and SCC9-re cells with stable expression of a miR-2392 sponge. **C**, Transfection of CAL-27 and SCC-9 cells with miR-2392 mimic enhanced ROS production, whereas ROS production was relieved by stable expression of a miR-2392 sponge in CAL-27-re and SCC-9-re cells. **D**, Transfection with a miR-2392 mimic reduced ND2, ND4, ND5, CYTB, and COX1 mRNA expression in CAL-27 cells and ND4, CYTB, COX1, and COX2 in SCC-9 cells, but the ND2, ND4, ND5, CYTB, and COX1 mRNA levels in CAL-27-re cells and the ND4, CYTB, COX1, and COX2 levels in SCC-9-re cells were upregulated by stable expression of a miR-2392 sponge. **E**, The expression levels of the proteins encoded by the genes mentioned in **D** were further confirmed by Western blotting. HK2 and PKM2 were upregulated in CAL-27 and SCC-9 cells upon transfection with the miR-2392 mimic but were downregulated in CAL-27-re and SCC-9-re cells stably expressing the miR-2392 sponge. **F**, Lactate production was enhanced in CAL-27 and SCC-9 cells by transfection with miR2392 mimic but was downregulated in CAL-27-re and SCC-9-re cells with stable expression of a miR-2392 sponge. Ncm, negative control for miR-2392 mimic; NCs, negative control for miR-2392 sponge. *, $P < 0.01$; **, $P < 0.001$, one-way ANOVA, followed by Dunnett's tests for multiple comparisons.



target sites cloned downstream of the promoter and upstream of the luciferase gene-mediated transcription repression in the nucleus, whereas 5'-mut miR-2392 lost the effect, which could be reversed by reverting the target sequences in the reporter to restore base pairing (Fig. 4F).

To further evaluate the necessity of AGO2 protein for inhibiting mitochondrial gene transcription via interaction with miR-2392, we used siRNAs to knock down AGO2 expression (Supplementary Fig. S6C) along with miR-2392 mimic addition in CAL-27 and SCC-9 cells. Knockdown of AGO2 caused a more than a 2-fold increase in miR-2392 target mtDNA-encoded genes expression and attenuated the inhibition of miR-2392 on target genes (Fig. 4G and H; Supplementary Fig. S6D and S6E). In addition, the occupancy of miR-2392 was significantly decreased in the mtDNA binding region by AGO2 knockdown (Fig. 4I), which was consistent with luciferase assay (Fig. 4J). Together, these results suggest that the AGO2-miR-2392 interaction is potentially required to inhibit mitochondrial gene transcription, similar to its requirement in the nucleus (20).

miR-2392 regulates cisplatin sensitivity in tongue squamous cell carcinoma xenografts

To further confirm the relationship between miR-2392 and metabolic balance in the regulation of cisplatin resistance, we established TSCC xenografts to investigate miR-2392 function *in vivo*. CAL-27 cells with stable expression of miR-2392 (Supplementary Fig. S7A and S7B) showed enhanced tumor growth in the presence of cisplatin and fewer apoptotic cells whereas the miR-2392 sponge had a reverse effect on CAL-27 xenografts (Fig. 5A–C; Supplementary Fig. S7C). We also found that after cisplatin treatment the expression levels of ND2, ND4, ND5, CYTB, and COX1 (Fig. 5D) were downregulated but those of HK2 and PKM2 (Fig. 5E) were upregulated in CAL-27 xenografts that stably expressed miR-2392, but the miR-2392 sponge increased targeted mtDNA-encoded genes whereas HK2 and PKM2 was downregulated in CAL-27-re xenografts (Fig. 5D and E). In addition, PCNA expression was not found to be significantly changed in each group, indicating that the influence of miR-2392 was not secondary to impaired proliferation (Supplementary Fig. S7D and S7E). These results suggest that miR-2392 overexpression inhibits apoptosis and cisplatin sensitivity *in vivo* by partially regulating mitochondrial gene expression and reprogramming metabolic balance.

Low miR-2392 expression and high ND4, CYTB, and COX1 expression are associated with chemosensitivity and favorable patient prognosis

To evaluate the clinical relevance of miR-2392 and the expression of its commonly targeted mitochondrial genes, ND4, CYTB, and COX1, in CAL-27 and SCC-9 cells with regard to chemosensitivity and patient prognosis in TSCC. We performed a retrospective analysis of TSCC samples from 115 patients. ISH demonstrated that miR-2392 expression was lower and IHC staining showed higher ND4, CYTB, and COX1 expression in chemosensitive TSCC tumors than in resistant tumors (Fig. 6A). Consequently, chemosensitive TSCC cells had a higher percentage of apoptotic cells than resistant cells (Fig. 6A). There was a significant difference in the expression profiles of chemosensitive and resistant TSCC tumors, as determined by the percentage of positive cells (Fig. 6B). Additionally, a Spearman order correlation analysis showed that miR-2392 expression was inversely correlated with ND4, CYTB, and COX1 levels (Fig. 6C).

Next, we analyzed the association of miR-2392, ND4, CYTB, and COX1 expression with TSCC patients' clinicopathological characteristics (Supplementary Table S4). No significant correlation was observed between miR-2392, ND4, CYTB, and COX1 expression and sex, age, lymph node status, or clinical stage. However, miR-2392, ND4, CYTB, and COX1 expression were significantly associated with chemoresistance. Moreover, the cumulative survival rate at 60 months was 42.64%, 44.62%, 45.21%, or 46.38% in patients with low miR-2392 expression or high ND4, CYTB, or COX1 expression, respectively; this rate was only 23.40%, 22.00%, 16.67%, or 17.39% in those with high miR-2392 expression or low ND4, CYTB, or COX1 expression, respectively (Supplementary Table S4). A univariate Cox regression analysis indicated that patients with TSCC with low miR-2392 expression levels or high ND4, CYTB, and COX1 levels had a longer overall survival (OS; Supplementary Table S4; Fig. 6D). Furthermore, a multivariate Cox regression analysis revealed that low-level miR-2392 expression and high-level ND4 and COX1 expression was an independent prognostic factor for good OS in patients with TSCC (Supplementary Table S5). We also confirmed that the commonly targeted mitochondrial gene had higher expressions in the primary cultured cells from chemosensitive patients comparing with that in chemoresistant ones (Fig. 6E). Interestingly, TCGA RNA-sequencing data also identified higher ND4, CYTB, and COX1 expression levels, which were associated with increased OS in five cancer types, including pancreatic adenocarcinoma, liver hepatocellular carcinoma, adrenocortical

Figure 3.

mitomiR-2392 partially regulates mitochondrial gene transcription. **A**, Real-time PCR following transcription inhibition by actinomycin-D treatment in CAL27 and SCC-9 cells transfected with miR-2392 mimics or its negative control. The ratio of individual MT-mRNA in group with transfection of mimics to that transfected with negative control was calculated at each time point. The percentage of RNA change with respect to time zero is also shown. **B**, Circos plot showing the free energy and binding sites between miR-2392 and the mitochondrial genome. The outer track shows the H-strand, whereas the inner track shows the L-strand. Red arrow, the most likely binding sites at 4379 to 4401 of mtDNA. **C**, RNAhybrid analysis showing the alignment of miR-2392 with the mtDNA H-strand, overlapping at 4379 to 4401. **D**, WebLogo analysis revealed that the targeted region of the H-strand is highly conserved in six primates. **E**, Alignment of mutant miR-2392 mimic with overlapping of the H-strand of mtDNA (mismatched bases underlined). **F**, ND2, ND4, ND5, CYTB, and COX1 mRNA expression affected by miR-2392 mimic and mutant miR-2392 mimic (3' mut and Mid-mut) in CAL-27 cells. Mitochondrial miR-513b and miR-1290 without an optimal binding site within mtDNA were selected as the controls. **G**, Northern blotting results demonstrating intramitochondrial localization of miR-2392; 12S rRNA served as the mitochondrial internal control and U6 as the internal control for total RNA analysis (left). FISH indicated that miR-2392 mainly overlaid with the mitochondria in CAL-27 cells (right). Colocalization coefficient (R) = 0.59. Scale bar, 3 μ m. *, $P < 0.01$; **, $P < 0.001$, one-way ANOVA, followed by Dunnett's tests for multiple comparisons.

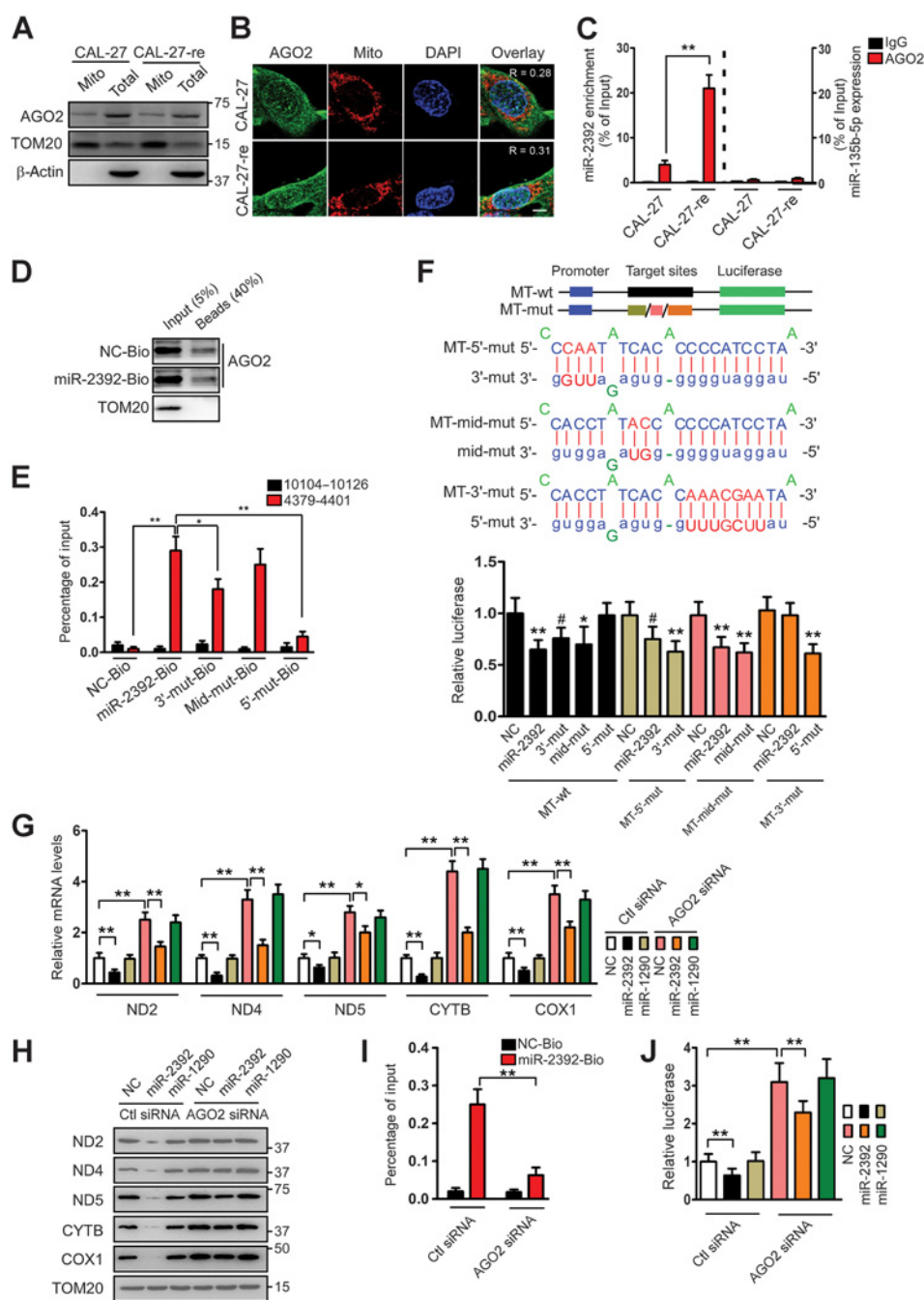


Figure 4. mitomiR-2392 regulates mitochondrial gene transcription associated with AGO2. **A**, Western blotting shows the presence of AGO2 in the mitochondria. **B**, Immunofluorescence staining indicates that a portion of AGO2 overlaid with mitochondria. Scale bar, 3 μ m. $R = 0.28$ and 0.31 in CAL-27 and CAL27-re cells, respectively. **C**, RNA immunoprecipitation demonstrated that miR2392 but not miR-135b-5p was coimmunoprecipitated with AGO2 in mitochondria, and more miR-2392 was coimmunoprecipitated from mitochondria of CAL-27-re cells. **D**, AGO2 coimmunoprecipitated with biotin-labeled miR-2392 and its negative control in mitochondria of CAL-27 cells. Five percent input and 40% magnetic beads were analyzed by Western blot analysis. **E**, qPCR was performed to detect enrichment of miR-2392 in the specific regulatory region (4379–4401) of mtDNA, whereas mutation of miR-2392 decreased the occupancy of this region in CAL-27 cells. **F**, miR-2392 and its mutants (3' mut and Mid-mut) but not 5' mut repressed the reporter containing miR-2392 target sites. The mutant miR-2392 target sites in the reporter weakened the effect, which could be restored with the corresponding mutant miR-2392 that reestablished the required base-pairing interactions. **G** and **H**, AGO2 knockdown attenuated the inhibition of miR-2392 on its targeted mitochondrial genes expression in CAL-27 cells. **G**, mRNA expression; **H**, change of protein levels. Cells were transfected with AGO2 siRNA, along with miR-2392 mimic. **I**, AGO2 knockdown decreased the enrichment of miR-2392 in the specific regulatory region (4379–4401) of mtDNA in CAL-27 cells. **J**, AGO2 knockdown increased the corresponding luciferase reporters in CAL-27 cells. **C**, **F**, and **I**, #, $P < 0.01$; *, $P < 0.01$; **, $P < 0.001$, two-tailed Student *t* tests; **E**, **G**, and **J**, *, $P < 0.01$; **, $P < 0.001$, one-way ANOVA, followed by Dunnett's tests for multiple comparisons.

Downloaded from <http://aacrjournals.org/cancerres/article-pdf/79/6/1069/2187525/1069.pdf> by guest on 27 August 2022

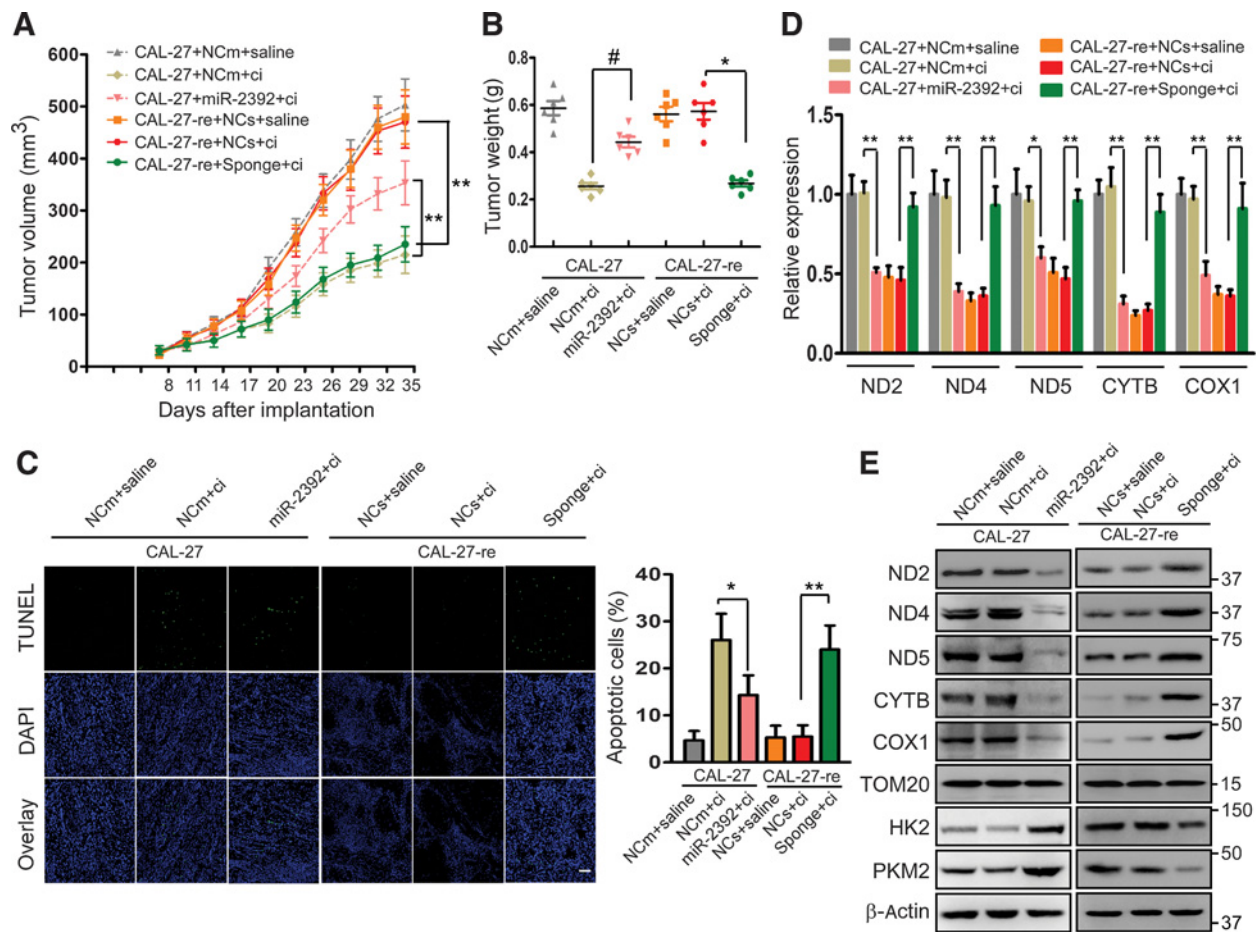


Figure 5. miR-2392 regulates tumor growth in CAL-27 and CAL-27-re cells xenografts in BALB/c-nu mice under cisplatin treatment. **A**, Growth curves for CAL-27 and CAL-27-re tumors treated with saline or cisplatin. BALB/c-nu mice bearing either CAL-27 cells with stable expression of miR-2392 or its control (NCm) or CAL-27-re cells with stable expression of miR-2392 sponge or its corresponding control (NCs; n = 6 for each group). **B**, Tumor weights in each group. **C**, Apoptosis was detected via a TUNEL assay. For the TUNEL assay, n = 24 slices from six xenograft tumors were sampled per group. Bar, 20 μm. **D**, qRT-PCR detection of ND2, ND4, ND5, CYTB, and COX1 mRNA expression per group. **E**, Western blotting showed that ND2, ND4, ND5, CYTB, and COX1 were reduced in the stable miR-2392 expression group, whereas HK2 and PKM2 were upregulated. miR-2392 sponge in CAL-27-re calls had a reverse effect. **A**, **, P < 0.001, two-way ANOVA, followed by Bonferroni's posttest; **B**, **D**, and **C**, #, P < 0.05; *, P < 0.01; **, P < 0.001, two-tailed Student t tests.

carcinoma, kidney chromophobe, and low-grade glioma (Fig. 6F). Together, these data suggest that miR-2392 expression may inversely correlate with chemosensitivity and OS, whereas its direct transcriptional targets, ND4, CYTB, and COX1, are associated with increased chemosensitivity and OS in patients with TSCC.

Discussion

Chemoresistance is a major obstacle to the successful application of chemotherapy for the treatment of malignant disease and has been shown to be caused by multiple mechanisms (40). Ongoing studies have revealed that inhibition of OXPHOS along with enhanced glycolysis contribute to chemoresistance (3, 5) and the molecular mechanisms underlining the metabolic reprogramming of cancer cells are complicated (1, 41). Among these studies, miRNAs-mediated gene silencing pathways have been studied extensively and multiple epige-

netic and posttranscriptional mechanisms have been identified to attribute to chemoresistance (42). In this study, for the first time, analysis of cell lines and surgically removed tumors contributes to our understanding of the molecular mechanism(s) underlying chemoresistance of carcinoma cells. This effect is mediated by an upregulation of mitomiRNA-2392, which reprograms cell metabolism including OXPHOS down-regulation and glycolysis upregulation, through partial regulation of mitochondrial transcription (Fig. 7).

Gene expression regulation by noncoding RNAs (ncRNA) has become a new paradigm in biology. A few studies reported the role of miRNAs in direct regulation of gene transcription. Computational methods have been developed to identify potential miRNA target sites within gene promoters. miRNAs complementary to gene promoters are potent silencers (18–20) and activators (17) of target gene expression *in cis* (19) and *in trans* (18, 20) in mammalian cells. Although the precise mechanism of activating or silencing transcription remains unclear, it is clear that

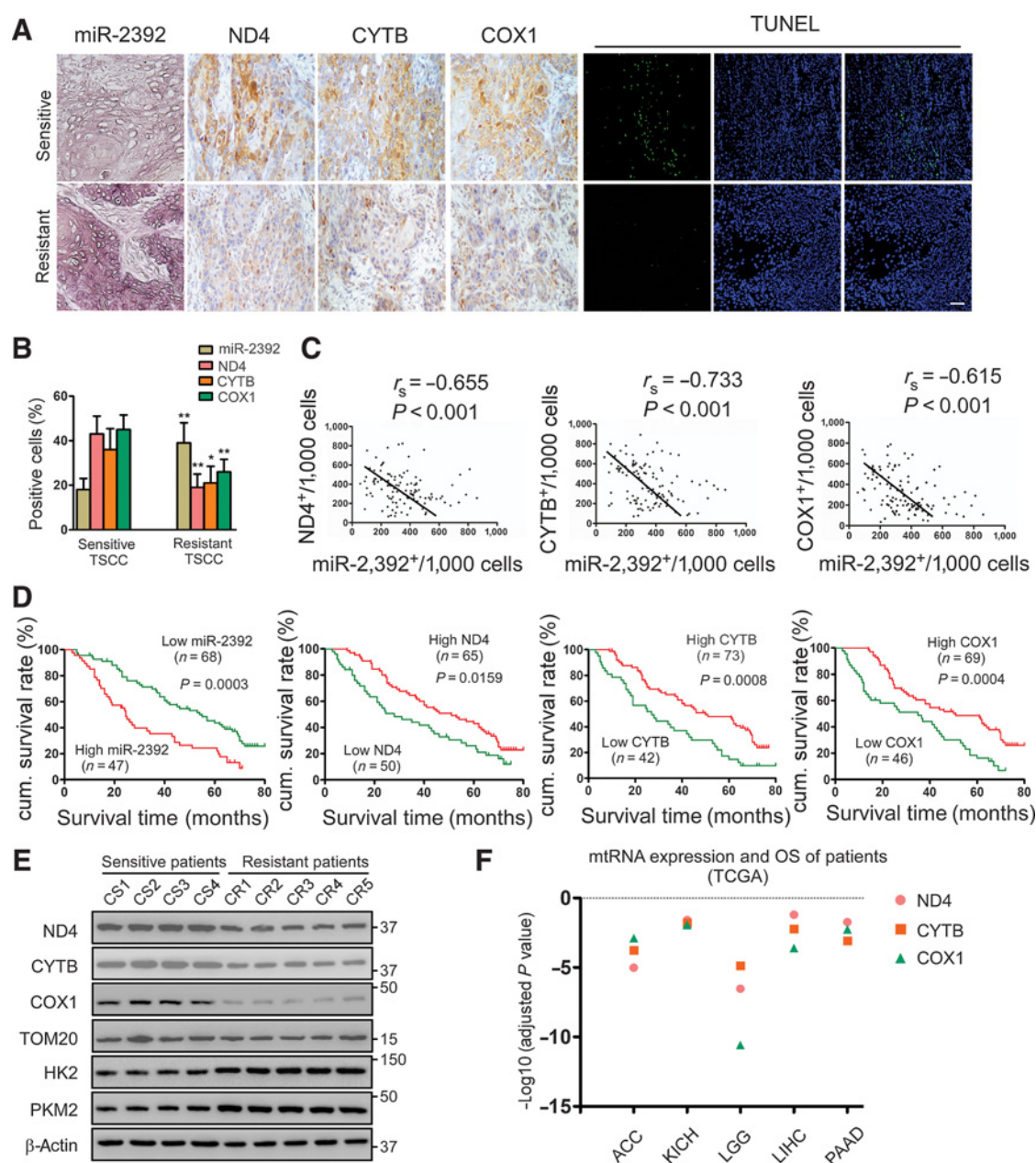


Figure 6.

Expression of miR-2392, ND4, CYTB, and COX1 is correlated with chemosensitivity and TSCC patient survival. **A**, miR-2392, ND4, CYTB, and COX1 expression and cell apoptosis were demonstrated in chemosensitive versus resistant TSCC tumors. Left, miR-2392 expression was analyzed using ISH ($\times 200$); ND4, CYTB, and COX1 expression were analyzed via IHC. Apoptosis was detected using a TUNEL assay. Bar, 20 μ m. **B**, Quantification of miR-2392, ND4, CYTB, and COX1 expression in chemosensitive versus resistant TSCC tumors. **C**, Associations between miR-2392 and ND4, CYTB, or COX1 expression in TSCC were analyzed via Spearman order correlation. **D**, Kaplan-Meier survival curves for patients with TSCC are plotted for miR-2392, ND4, CYTB, and COX1 expression, and survival differences were analyzed using a log-rank test. **E**, Western blotting showed that ND4, CYTB, and COX1 expression was reduced in primary cultured cells from chemoresistant patients, whereas HK2 and PKM2 were upregulated. **F**, Association of mtRNA expression levels with OS in multiple types of human cancer based on TCGA RNA sequencing data. ACC, adrenocortical carcinoma; KICH, kidney chromophobe; LGG, low-grade glioma; LIHC, liver hepatocellular carcinoma; PAAD, pancreatic adenocarcinoma. *, $P < 0.01$; **, $P < 0.001$; two-tailed Student t tests.

miRNAs can recognize and overlap nuclear gene promoters and regulate transcription. Our present study further explores the functions of the miRNA machinery in mitochondria. We found that one mitomiR, miR-2392 overlaps with specific sequences in

the H-strand body, but only partially regulates downstream gene transcription in the H-strand. Also, the downstream genes regulated by miR-2392 are different between two TSCC cell lines. There are several possible reasons. First, miRNAs mainly function

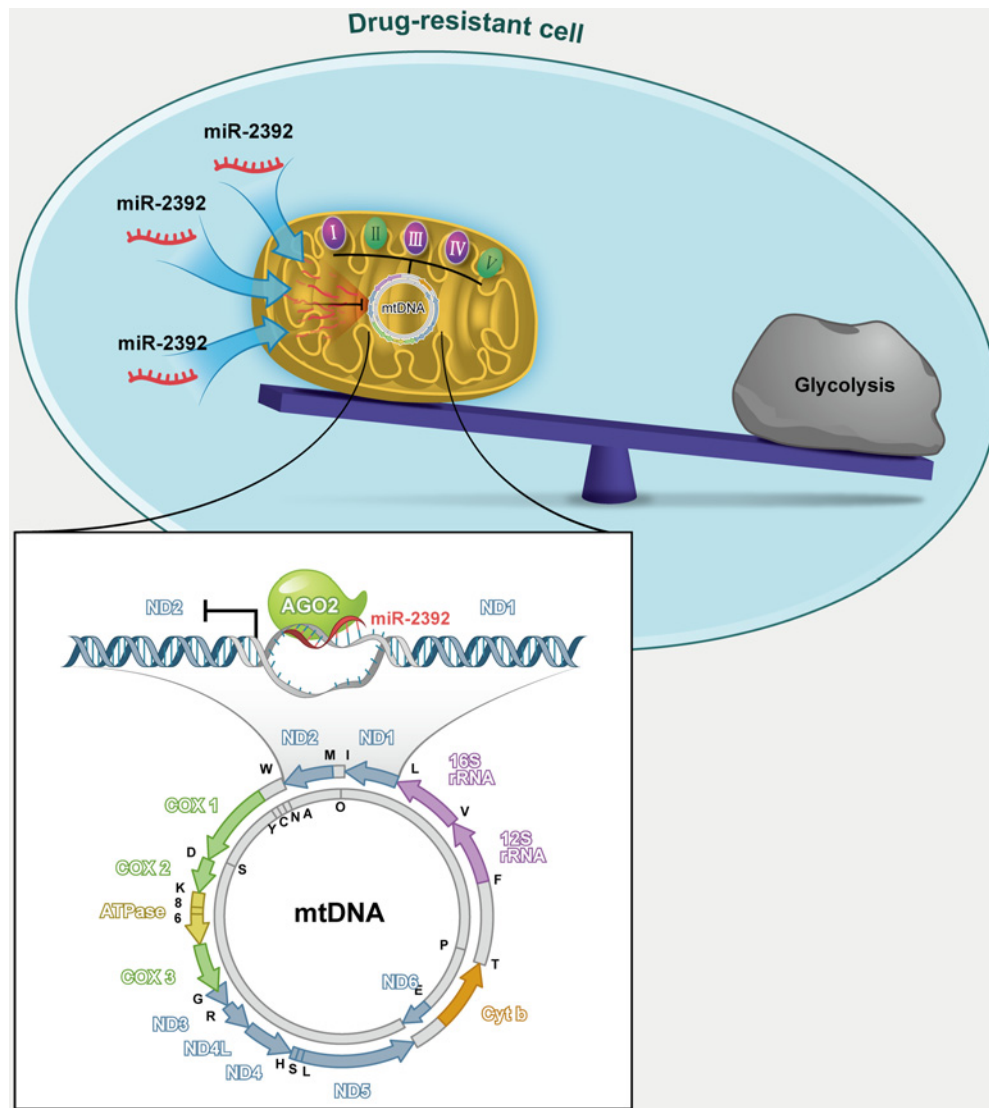


Figure 7. Model of how mitomiR miR-2392 determines chemoresistance and metabolic reprogramming by partially regulating transcription of the mitochondrial genome.

as micromanagers, and we cannot exclude the possibility that other mitomiRs that were not detected by the microarray are involved in the transcription, along with their undiscovered functions. Second, other mitomiRs may inhibit target mitochondrial mRNA translation but also stimulate a compensatory increase in synthesis of the H2 strand (22) and mitochondrial transcription. Third, although we did not find that miR-2392 had any effect on mitochondrial replication and transcription factor (POLRMT, TFB2M, and TFAM) expression, the mechanism of mammalian mitochondrial transcription and epigenetic modification remain controversial. The exact hierarchy of mitochondrial RNA processing (43), posttranscriptional regulation (44), and mtDNA methylation (45) may result in uneven steady-state abundances of polycistronic transcripts in mitochondria (44). We cannot absolutely exclude the possibilities that miR-2392 may regulate nuclear genes other than RGCC and STAT1 and indirectly influence these issues in mitochondria. Fourth, the AGO2-miR-

2392 complex was validated to bind mtDNA gene body instead of promoter in this study. Some evidence identified the recruitment of a particular molecule within gene bodies that is required to induce nuclear gene repression, such as H2A.Z (46) but little is known about its function in the mitochondria. Fifth, the single study to date that has examined the expression of the 13 mtRNAs based on TCGA RNA-sequencing data, also found differential expression of mtRNA across different cancer types, such as encoding subunits of Complex I and Complex IV and V (37). Sixth, miRNAs transcriptionally regulate nuclear gene expression under specific cellular conditions (17–20), and our data are consistent with previous studies showing that transcriptional regulation of miR-2392 is cell specific in our current cellular models.

Concerning target recognition by miRNAs, it has been reported that miRNAs do not require full complementarity to be active in transcriptional silencing (20), and we found that miR-2392 had a few mismatched bases with its target sequences. However, basic

base-pairing and binding energy are required because miR-2392 specifically binds to the mtDNA at region (4379–4401) rather than binding to a poorly matched binding site (10104–10126); another mitomiRNAs, miR-513b and miR-1290, did not show transcriptional activity. Moreover, other groups have reported the involvement of AGO2 in small RNA-induced transcriptional gene silencing (47). In a series of rigorously controlled experiments, we also found that mitomiR-2392 silences mtDNA transcription through an AGO2-dependent mechanism, even though other AGO2 binding elements may directly or indirectly modulate this phenomenon in our cellular system. Our results suggest that the principles of mitomiR function in mtDNA transcription are possibly consistent with the corresponding principles in the nucleus. However, other important questions await future studies, such as how AGO2 and miRNAs are able to selectively enter the mitochondria. Importantly, most nuclear DNA-encoded mitochondrial proteins do not contain any identifiable mitochondrial targeting sequences (25). Although 5S rRNA and tRNA can be actively imported into the mitochondria and other preliminary mitochondrial import assay indicates that multiple specific and nonspecific miRNAs were able to enter purified mitochondria without the need for ATP hydrolysis (25), we found that efficient entry of miR-2392 into the mitochondria could not be explained as a sequence-dependent manner, because similar enrichment of expression was detected after transfection of three types of mutant miR-2392 mimics. Therefore, how exactly miRNAs selectively enter the mitochondria remains elusive thus far. Another unaddressed issue is that miR-2392 shows no similar effect on a nuclear DNA fragment although it has a 17–19nt DNA complementary to miR-2392. We hypothesize that it might be the different secondary and tertiary structure between nuclear DNA and mitochondria DNA that leads to this difference. Given the completely opposite regulation of miRNAs between mitochondria and cytoplasm as the defect of GW182 along by induction of translational enhancement in the mitochondria (25), we speculate that the transcriptional modulation by miRNA requires other chaperones that may be differently expression between mitochondria and cytoplasm. Further exploration of the potential mechanism are needed.

Hallmarks of cancer, such as self-sufficiency in growth signals, sustained angiogenesis, tissue invasion, metastasis, and avoidance of immune surveillance, have been linked to metabolic changes (1). The molecular mechanisms that underlie the metabolic reprogramming of cancer cells are complex. Regulation of these processes and molecular switching that is involved in metabolic programming may have a dramatic effect on tumors, not only by limiting cancer cell-specific bioenergetic flow and anabolic reactions but also by reversing the neoplastic phenotype and hence stopping growth, inducing apoptosis, and/or blocking chemoresistance, angiogenesis, and invasion (1). Generally, a sufficiently large reduction in the levels of proteins encoded by mtDNA, will precipitate a drop in the rate of energy generation via respiration. In these cases, cancer cells can partially compensate by increasing flux through glycolysis (i.e., the Warburg effect). Ongoing studies have revealed the presence of a dynamic balance between aerobic glycolysis and mitochondria respiration-OXPHOS in cancer cells (5, 34). Disturbances in metabolic balance may be attributed to chemoresistance at several levels, which has widely been discussed (48). Many reports have examined changes in metabolic gene expression in cancer, but one study has examined the expression of the 13 mRNAs encoded by

the mitochondrial genome (37). Reznik and colleagues, realigned TCGA RNA-sequencing data and estimated the differential expression of mtRNA transcripts in tumor versus normal tissues for each of 13 cancer types with adequate numbers of tumor and normal samples. They found that the majority of cancer types have a tendency for lower levels of mtRNAs. More interestingly, they identified five cancer types in which higher mtRNA expression levels were associated with increased OS (37), including ND4, CYTB, or COX1, which has further identified the significant clinical relevance in our present study. We hope our study can echo similar findings by others which further investigate the clinical importance of expression and regulation of mtRNA.

In conclusion, our findings expand upon the current understanding of mitomiR and imply that the mitomiRNA triggers chemoresistance by reprogramming metabolism of carcinoma cells through partially regulating mitochondrial transcription with an AGO2-dependent manner rather than translation regulation. Moreover, evidence from mitomiR-2392 and the regulated mitochondrial genome strongly suggest that these molecules may have the ability in predicting chemosensitivity and patient clinical prognosis.

Disclosure of Potential Conflicts of Interest

No potential conflicts of interest were disclosed.

Authors' Contributions

Conception and design: S. Fan, T. Tian, G. Pan, S. Ferrone, B.A. Tannous, J. Li
Development of methodology: S. Fan, T. Tian, W. Chen, X. Lv, G. Pan, X. Lin
Acquisition of data (provided animals, acquired and managed patients, provided facilities, etc.): S. Fan, T. Tian, W. Chen, X. Lv, H. Zhang, G. Pan, Z. Ou, Z. Tu
Analysis and interpretation of data (e.g., statistical analysis, biostatistics, computational analysis): S. Fan, T. Tian, H. Zhang, S. Sun, G. Pan, Z. Ou, X. Lin, Z. Tu, B.A. Tannous
Writing, review, and/or revision of the manuscript: S. Fan, X. Lei, S. Sun, L. Cai, G. Pan, L. He, X. Wang, M.F. Perez, S. Ferrone, B.A. Tannous, J. Li
Administrative, technical, or material support (i.e., reporting or organizing data, constructing databases): S. Fan, G. Pan
Study supervision: G. Pan, S. Ferrone, J. Li

Acknowledgments

We are grateful to Michael Ho-Young Ahn and Yingjin Lin for critical reading of the manuscript. We appreciate Faya Liang and Sha Fu for their great help in analyzing the tissue slides. This work was supported by grants from NIH (R01DE028172 to S. Ferrone), National Natural Science Foundation of China (No. 81472521 to S. Fan; 81402251 to J.S. Li; 81502350 to X.B. Lv; 81672676 to J.S. Li; 81772890 to S. Fan), Guangdong Science and Technology Development Fund (2015A030313181 to S. Fan; 2016A030313352 to J.S. Li), Science and Technology Program of Guangzhou (201607010108 to S. Fan; 201803010060 to J.S. Li), Fundamental Research Funds for the Central Universities (16ykpy10 to S. Fan), National Clinical Key Specialty Construction Project for Department of Oral and Maxillofacial Surgery to S. Fan and J.S. Li, The Key Laboratory of Malignant Tumor Gene Regulation and Target Therapy of Guangdong Higher Education Institutes, Sun-Yat-Sen University (Grant KLB09001 to J.S. Li), Key Laboratory of Malignant Tumor Molecular Mechanism and Translational Medicine of Guangzhou Bureau of Science and Information Technology ([2013]163 to J.S. Li).

The costs of publication of this article were defrayed in part by the payment of page charges. This article must therefore be hereby marked *advertisement* in accordance with 18 U.S.C. Section 1734 solely to indicate this fact.

Received August 11, 2018; revised November 1, 2018; accepted January 10, 2019; published first January 18, 2019.

References

- Kroemer G, Pouyssegur J. Tumor cell metabolism: cancer's Achilles' heel. *Cancer Cell* 2008;13:472–82.
- Gatenby RA, Gillies RJ. Why do cancers have high aerobic glycolysis? *Nat Rev Cancer* 2004;4:891–9.
- Rodriguez-Enriquez S, Carreno-Fuentes L, Gallardo-Perez JC, Saavedra E, Quezada H, Vega A, et al. Oxidative phosphorylation is impaired by prolonged hypoxia in breast and possibly in cervix carcinoma. *Int J Biochem Cell Biol* 2010;42:1744–51.
- Ma WW, Jacene H, Song D, Vilardell F, Messersmith WA, Laheru D, et al. [18F]fluorodeoxyglucose positron emission tomography correlates with Akt pathway activity but is not predictive of clinical outcome during mTOR inhibitor therapy. *J Clin Oncol* 2009;27:2697–704.
- Leung EY, Kim JE, Askarian-Amiri M, Joseph WR, McKeage MJ, Baguley BC. Hormone resistance in two MCF-7 breast cancer cell lines is associated with reduced mTOR signaling, decreased glycolysis, and increased sensitivity to cytotoxic drugs. *Front Oncol* 2014;4:221. doi: 10.3389/fonc.2014.00221.
- Bonawitz ND, Clayton DA, Shadel GS. Initiation and beyond: multiple functions of the human mitochondrial transcription machinery. *Mol Cell* 2006;24:813–25.
- Asin-Cayuela J, Gustafsson CM. Mitochondrial transcription and its regulation in mammalian cells. *Trends Biochem Sci* 2007;32:111–7.
- Mick DU, Fox TD, Rehling P. Inventory control: cytochrome c oxidase assembly regulates mitochondrial translation. *Nat Rev Mol Cell Biol* 2011;12:14–20.
- Zollo O, Tiranti V, Sondheimer N. Transcriptional requirements of the distal heavy-strand promoter of mtDNA. *Proc Natl Acad Sci U S A* 2012;109:6508–12.
- Malarkey CS, Bestwick M, Kuhlwilms JE, Shadel GS, Churchill ME. Transcriptional activation by mitochondrial transcription factor A involves preferential distortion of promoter DNA. *Nucleic Acids Res* 2012;40:614–24.
- Bestwick ML, Shadel GS. Accessorizing the human mitochondrial transcription machinery. *Trends Biochem Sci* 2013;38:283–91.
- Yakubovskaya E, Mejia E, Byrnes J, Hambardjjeva E, Garcia-Diaz M. Helix unwinding and base flipping enable human MTERF1 to terminate mitochondrial transcription. *Cell* 2010;141:982–93.
- Ramachandran A, Basu U, Sultana S, Nandakumar D, Patel SS. Human mitochondrial transcription factors TFAM and TFB2M work synergistically in promoter melting during transcription initiation. *Nucleic Acids Res* 2017;45:861–74.
- Lodeiro MF, Uchida A, Bestwick M, Moustafa IM, Arnold JJ, Shadel GS, et al. Transcription from the second heavy-strand promoter of human mtDNA is repressed by transcription factor A in vitro. *Proc Natl Acad Sci U S A* 2012;109:6513–8.
- Carthew RW, Sontheimer EJ. Origins and Mechanisms of miRNAs and siRNAs. *Cell* 2009;136:642–55.
- Chekulaeva M, Filipowicz W. Mechanisms of miRNA-mediated post-transcriptional regulation in animal cells. *Curr Opin Cell Biol* 2009;21:452–60.
- Place RF, Li LC, Pookot D, Noonan EJ, Dahiya R. MicroRNA-373 induces expression of genes with complementary promoter sequences. *Proc Natl Acad Sci U S A* 2008;105:1608–13.
- Sepramaniam S, Ying LK, Armugam A, Wintour EM, Jeyaseelan K. MicroRNA-130a represses transcriptional activity of aquaporin 4 M1 promoter. *J Biol Chem* 2012;287:12006–15.
- Kim DH, Saetrom P, Snove O Jr, Rossi JJ. MicroRNA-directed transcriptional gene silencing in mammalian cells. *Proc Natl Acad Sci U S A* 2008;105:16230–5.
- Younger ST, Corey DR. Transcriptional gene silencing in mammalian cells by miRNA mimics that target gene promoters. *Nucleic Acids Res* 2011;39:5682–91.
- Bandiera S, Ruberg S, Girard M, Cagnard N, Hanein S, Chretien D, et al. Nuclear outsourcing of RNA interference components to human mitochondria. *PLoS One* 2011;6:e20746.
- Das S, Ferlito M, Kent OA, Fox-Talbot K, Wang R, Liu D, et al. Nuclear miRNA regulates the mitochondrial genome in the heart. *Circ Res* 2012;110:1596–603.
- Kren BT, Wong PY, Sarver A, Zhang X, Zeng Y, Steer CJ. MicroRNAs identified in highly purified liver-derived mitochondria may play a role in apoptosis. *RNA Biol* 2009;6:65–72.
- Sripada L, Tomar D, Prajapati P, Singh R, Singh AK, Singh R. Systematic analysis of small RNAs associated with human mitochondria by deep sequencing: detailed analysis of mitochondrial associated miRNA. *PLoS One* 2012;7:e44873.
- Zhang X, Zuo X, Yang B, Li Z, Xue Y, Zhou Y, et al. MicroRNA directly enhances mitochondrial translation during muscle differentiation. *Cell* 2014;158:607–19.
- Nouws J, Shadel GS. microManaging mitochondrial translation. *Cell* 2014;158:477–8.
- Sun L, Yao Y, Liu B, Lin Z, Lin L, Yang M, et al. MiR-200b and miR-15b regulate chemotherapy-induced epithelial-mesenchymal transition in human tongue cancer cells by targeting BMI1. *Oncogene* 2012;31:432–45.
- Valente MJ, Henrique R, Costa VL, Jeronimo C, Carvalho F, Bastos ML, et al. A rapid and simple procedure for the establishment of human normal and cancer renal primary cell cultures from surgical specimens. *PLoS One* 2011;6:e19337.
- Wang JX, Jiao JQ, Li Q, Long B, Wang K, Liu JP, et al. miR-499 regulates mitochondrial dynamics by targeting calcineurin and dynamin-related protein-1. *Nat Med* 2011;17:71–8.
- Fan S, Liu B, Sun L, Lv XB, Lin Z, Chen W, et al. Mitochondrial fission determines cisplatin sensitivity in tongue squamous cell carcinoma through the BRCA1-miR-593-5p-MFF axis. *Oncotarget* 2015;6:14885–904.
- Zhong LP, Zhang CP, Ren GX, Guo W, William WN Jr., Sun J, et al. Randomized phase III trial of induction chemotherapy with docetaxel, cisplatin, and fluorouracil followed by surgery versus up-front surgery in locally advanced resectable oral squamous cell carcinoma. *J Clin Oncol* 2013;31:744–51.
- Zhang Y, Maurizi MR. Mitochondrial ClpP activity is required for cisplatin resistance in human cells. *Biochim Biophys Acta* 2016;1862:252–64.
- Jeon JH, Kim DK, Shin Y, Kim HY, Song B, Lee EY, et al. Migration and invasion of drug-resistant lung adenocarcinoma cells are dependent on mitochondrial activity. *Exp Mol Med* 2016;48:e277.
- Zhou Y, Tozzi F, Chen J, Fan F, Xia L, Wang J, et al. Intracellular ATP levels are a pivotal determinant of chemoresistance in colon cancer cells. *Cancer Res* 2012;72:304–14.
- Chen J, Yao D, Li Y, Chen H, He C, Ding N, et al. Serum microRNA expression levels can predict lymph node metastasis in patients with early-stage cervical squamous cell carcinoma. *Int J Mol Med* 2013;32:557–67.
- Li J, Li T, Lu Y, Shen G, Guo H, Wu J, et al. MiR-2392 suppresses metastasis and epithelial-mesenchymal transition by targeting MAML3 and WHSC1 in gastric cancer. *FASEB J* 2017;31:3774–86.
- Reznik E, Wang Q, La K, Schultz N, Sander C. Mitochondrial respiratory gene expression is suppressed in many cancers. *Elife* 2017;6. doi: 10.7554/eLife.21592.
- Panasyuk G, Espeillac C, Chauvin C, Pradelli LA, Horie Y, Suzuki A, et al. PPAR γ contributes to PKM2 and HK2 expression in fatty liver. *Nat Commun* 2012;3:672. doi: 10.1038/ncomms1667.
- DeBalsi KL, Hoff KE, Copeland WC. Role of the mitochondrial DNA replication machinery in mitochondrial DNA mutagenesis, aging and age-related diseases. *Ageing Res Rev* 2017;33:89–104.
- Guerra F, Arbini AA, Moro L. Mitochondria and cancer chemoresistance. *Biochim Biophys Acta* 2017;1858:686–99.
- Kroemer G, Galluzzi L, Brenner C. Mitochondrial membrane permeabilization in cell death. *Physiol Rev* 2007;87:99–163.
- Garofalo M, Croce CM. MicroRNAs as therapeutic targets in chemoresistance. *Drug Resist Updat* 2013;16:47–59.
- Xu F, Ackerley C, Maj MC, Addis JB, Levandovskiy V, Lee J, et al. Disruption of a mitochondrial RNA-binding protein gene results in decreased

- cytochrome b expression and a marked reduction in ubiquinol-cytochrome c reductase activity in mouse heart mitochondria. *Biochem J* 2008;416:15–26.
44. Rorbach J, Minczuk M. The post-transcriptional life of mammalian mitochondrial RNA. *Biochem J* 2012;444:357–73.
 45. Mehta M, Ingerslev LR, Fabre O, Picard M, Barres R. Evidence suggesting absence of mitochondrial DNA methylation. *Front Genet* 2017;8:166. doi: 10.3389/fgene.2017.00166.
 46. Lashgari A, Millau JF, Jacques PE, Gaudreau L. Global inhibition of transcription causes an increase in histone H2A.Z incorporation within gene bodies. *Nucleic Acids Res* 2017;45:12715–22.
 47. Janowski BA, Huffman KE, Schwartz JC, Ram R, Nordsell R, Shames DS, et al. Involvement of AGO1 and AGO2 in mammalian transcriptional silencing. *Nat Struct Mol Biol* 2006;13:787–92.
 48. Rahman M, Hasan MR. *Cancer Metabolism and Drug Resistance. Metabolites* 2015;5:571–600.